USE OF MAGNESIAN-DOLOMITE MIXTURES IN STEEL-MELTING FURNACE HEARTHS AND THE MECHANISM OF THEIR WEAR IN SERVICE. 1. STUDY OF ANKERHARTH REFRACTORIES

T. I. Shchekina,[1] E. N. Gramenitskii,[1] A. M. Batanova,[1] T. A. Kurbyko,[1] A. V. Likhodievskii,[1] B. N. Grigor'ev,[1] and A. N. Pyrikov[1]

Translated from *Novye Ogneupory*, No. 10, pp. 45 – 54, October, 2006.

Original article submitted June 28, 2006.

The results of mineralogical-petrographic analysis of Ankerharth magnesian-dolomite refractory mixtures used in the hearths of steel-melting furnaces are described. The regularities of changes in their phase and chemical compositions are identified and the mechanism of their wear in service at the Omutninskii Metallurgical Works is considered.

Refractory materials have a very significant role in ensuring reliable and safe performance of metallurgical plants and influence the quality and production cost of steel. Recently, steel-melting furnaces in the nonferrous sector have tended to grow in sizes and their service temperatures have increased; consequently, requirements imposed on the quality of melting have grown as well. Therefore, the significance of high-grade non-molded refractories has also grown, since they have to satisfy more severe operating conditions. The main properties of a refractory ramming mixture are the constancy of its volume at high temperatures, corrosion resistance, and wear resistance. Correct ramming of a furnace hearth increases the efficiency of the steel-melting furnace and extends the service life of its working chamber. Identification of negative factors affecting the service life of refractories, studying the mechanism of their wear, and selecting refractories with optimal properties remain topical issues. In this context, we have performed a comparative study of the wear mechanism of open-hearth furnace bottoms rammed by magnesian-dolomite mixtures of the Ankerharth and Jehearth grades supplied by foreign producers. The results of these studies are summarized in two papers. The first paper describes the study of the wear mechanism of Ankerharth materials produced by RHI AG (Austria) sampled after their service in furnaces at the Omutninskii Metallurgical Works.

The main line of our research was studying chemical corrosion of refractories, which is one of the most significant factors influencing their resistance. The latter depends not only on the chemical and mineral composition of rammed lining and the composition of metallurgical melts, but also on the method and quality of ramming the furnace chamber and the location of refractories in the furnace hearth.

The main purpose of this study was to investigate diffusion zonality arising in ramming mixtures when they react with molten metal and slag and to analyze the effect of changes in the chemical and mineralogical compositions of refractory materials in service on their resistance. To solve this problem we analyzed the chemical and phase composition, texture, and structure of samples taken from an open-hearth furnace bottom before and after service correlated to different zones formed in the samples in the course of reactions between refractory materials and molten metal and slag. Our study was based on the principles of the metasomatic zonality theory developed by D. S. Korzhinskii [1] for natural processes and on our own studies of reactions between periclase-chromite refractories and nickel converter matte [2] and between mineral rocks and magmatic melts [3 – 5]. Some earlier mineralogical-petrographic studies of the composition and structure of periclase and dolomite refractories and ramming mixtures are summarized in works of L. I. Karyakin [6] and D. S. Belyankin with colleagues [7].

INVESTIGATION METHODS

The considered grades of refractory mixtures sampled after their service in open-hearth furnaces mainly constitute densely sintered hard materials. Samples from sites adjunct

[1] M. V. Lomonosov Moscow State University, Moscow, Russia; OgneuporTreidGrupp JSC, Russia.

to metallurgical melt had a zonal structure. Samples that were far from the contact with the melt were represented by powders consisting of fragments ranging from fractions of a millimeter to 5 – 8 mm. The samples with clearly expressed zonality were cut perpendicularly to their contact with the reaction (working) zone. Then they were used to prepare transparent and polished-transparent sections, which were analyzed using a polarizing microscope in incident and reflected light. The samples were also analyzed using Camscan 4DV and Camscan MV 2300 scanning electron microscopes. The structure and the qualitative phase composition were recorded as electronic images (photos) in backward scattered electrons (BSE). Local x-ray diffraction analysis of minerals was carried out using the LINK analyzers working with the electron microscopes, as well as Camebax SX50 and Camebax MBX microprobes. The reaction zones of the samples were also investigated in characteristic radiation of the main elements (Si, Al, Ca, Fe). The microprobe analysis of each phase provided a precise identification of this phase and its specific composition. Analysis using an electron scanning beam on a square with a chosen side equal to a few tens of microns yielded the gross composition of the sample sites. Silicate chemical analysis was performed for several samples of initial refractories before service and the reaction zones after service, which, in particular, provided an estimate of changes in the ratio of bivalent to trivalent iron split by the sample zones.

To identify the phase composition and to have an approximate estimate of the number of phases in a sample, x-ray phase analysis of initial refractories and of some refractories after service was implemented on a DRON diffractometer. The identification of phases was performed by computerized data processing using special software for x-ray phase analysis and the PDF-2 international database.

The norm of refractory samples before service and after service (split by zones) was determined using P. Niggley's molecular-norm method accepted in petrology. The results of petrochemical calculations made it possible to compare the phases and their quantitative ratios in the reaction zones obtained from the gross compositions of the sample and data obtained by electron microscopy and microprobes.

EXPERIMENTAL RESULTS AND DISCUSSION

Composition and Structure of Initial Ankerharth Mixtures

Ankerharth magnesian-dolomite mixtures produced by RHI AG are produced in several grades intended for application in various sites of an open-hearth furnace bottom. All mixtures are friable, gray-colored, powder-like materials consisting of particles of different sizes. The basis of the mixture is a powder whose 30 – 40 vol.% is represented by solid fragments of dark gray and light gray colors and of size from 1 to 8 mm, mainly 3 – 5 mm. Different grades of refractory mixtures have similar compositions and, according to the standard, differ from each other by no more than 2.3% MgO, 0.4% SiO_2, 2% CaO, and 0.7% FeO. The content of Al_2O_3 in the mixtures is equal (Table 1). The Ankerharth TLS2 mixture for the blow zone contains a coarser fraction (up to 8 mm), in contrast to Ankerharth SB25 intended for the walls and the banks. Considering the similarity of their chemical and phase compositions, we performed silicate analysis (Table 1) and x-ray phase analysis of just one grade, namely Ankerharth TLS2, which was the initial mixture for a series of hearth samples. Large fragments (~5 mm) were taken from this mixture as well, in order to analyze all of its phases using a microprobe.

The data obtained in gross silicate analysis of Ankerharth TLS2 given in Table 1 differ from the standard (specification) parameters by a higher content of MgO and SiO and a lower content of CaO. This shows that the composition of refractory mixtures produced by the company probably does not fully meet the specified standard. Comparing refractory mixtures before and after service, we decided to use the standard compositions as reference data.

Silicate analysis separately performed for the coarse and pulverized fractions of Ankerharth TLS2 (sample M16) indicates that their most significant difference is the ratio of MgO to CaO. The pulverized fraction is rich in CaO and the coarse fragments are rich in MgO. The composition of the fragments, in turn, is also heterogeneous with respect to various components. The analyzed large fragments of sample M16 contain 7% more MgO, 2% more SiO, 2.4% more FeO, and 15% less CaO than the standard composition of the material. These differences are presumably due to the fact that the composition of large fragments is not equivalent to the gross composition of the material in general.

According to electron microscopy data, the structure of large fragments of initial Ankerharth TLS2 has an irregular granularity (Fig. 1); its major part is made up of coarse-grained aggregates consisting, to an extent of 80 – 90%, of periclase grains $(Mg_{0.98}Fe_{0.02})_{1.00}O$ with a small quantity (2 – 5%) of lime. The spaces between the periclase grains are filled with tricalcium ferrite $(Ca_{2.8}Mg_{0.1}Mn_{0.1}P_{0.1})_{3.1}(Fe_{2.0}Al_{0.2})_{2.2}O_6$, which amount to 5 – 8% of the volume of the aggregates (Fig. 1*b*) and small quantities of calcium silicate and aluminate. These aggregates are presumably the products of magnesite firing. The smaller part is represented by close-grained aggregates, which, in addition to periclase, contain a large quantity of calcium phases in the form of lime and portlandite, which presumably are the products of dolomite firing.

The norm of initial refractories calculated using the standard data and the results of gross chemical composition of the materials (Table 1) mainly corroborates the results of studying the phase composition using electron microscopes and microprobes. Similar estimates of the mineral composition and the number of phases are obtained by x-ray phase analysis, which indicates that the material contains 89.5% periclase, 8.9% lime, 0.6% portlandite $Ca(OH)_2$, and 1% quartz. Calcium ferrites and aluminates have not been identi-

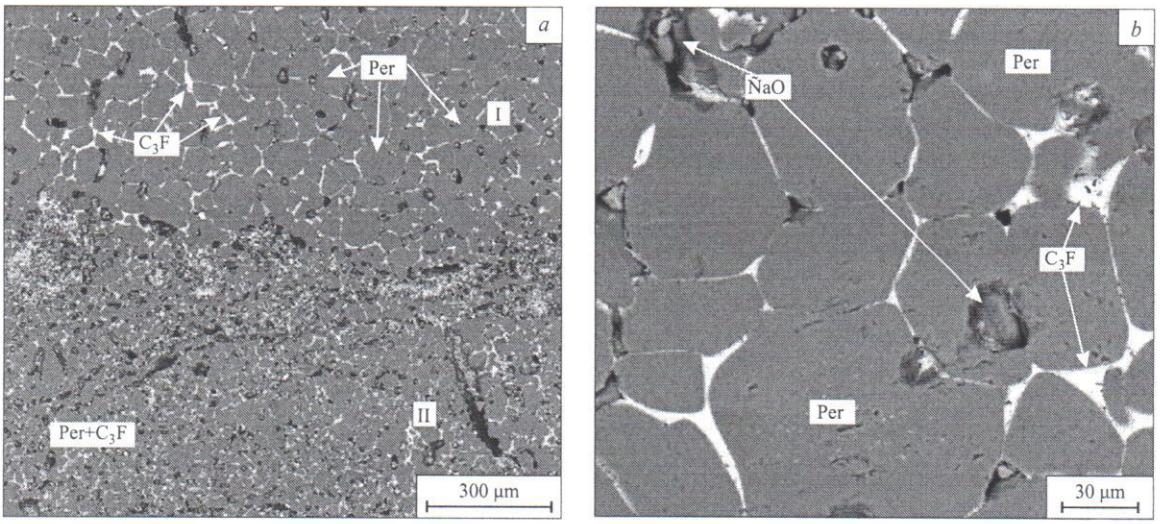

Fig. 1. General view of refractory mixture Ankerharth TLS2 (sample M16). *a*) Fragments of two types with different granularity: coarse-grained (*I*) and fine-grained (*II*); *b*) the structure of a coarse-grained area in a fragment of size 4 – 5 mm; the basis consists of periclase grains (Per) of dark gray color in BSE bonded by three-calcium ferrite (C_3F), white-colored in BSE; the pores are filled with loose lime mixtures (CaO).

TABLE 1. Gross Chemical Compositions and Norms of Initial Refractories Ankerharth SB25 and Ankerharth TLS2 before Service and after Service Split by Reaction Zones in Samples M14-1

Parameters	Material grade						
	Ankerharth SB25	Ankerharth TLS2					
Method of analysis	Specifications		Silicate*1	Microprobe*2			
Zone	0*3	0	0	1	2	3	4
Distance from the contact, mm	>20	>20	>20	103 – 518	4.53 – 510	3.53 – 54.5	03 – 53.5
Mass content of main components, %							
SiO_2	0.6	0.6	1.47	1.94	7.81	2.22	6.41
TiO_2	—	—	0.01	0.46	0.28	0.3	0.35
Al_2O_3	0.3	0.3	0.4	3.02	1.51	0.85	1.56
Fe_2O_3	2.91	3.62	7.83	—	—	—	—
FeO	—	—	0.33	15.68	20.5	32.01	50.21
MnO	—	—	0.28	1.67	3.37	4.44	4.29
MgO	77.15	74.37	81.43	43.37	51.81	55.86	23.3
CaO	19.04	21.1	14.25	33.86	14.56	4.32	13.58
CaO/SiO_2	31.73	35.16	7.21	17.45	1.86	1.95	2.12
Phase content (norm analysis), mol.%							
MgO	83.00	81.06	86.41	54.45	—	—	—
(Mg, Fe)O	—	—	—	—	63.44	71.74	24.47
Ca_2SiO_4	—	—	3.21	—	19.04	5.62	18.46
Ca_3SiO_5	1.74	1.73	—	6.34	—	—	—
$Ca_3Al_2O_6$	1.04	0.65	—	—	—	—	—
$Ca_3Fe_2O_6$	3.90	3.80	4.97	19.84	—	—	—
$Ca_3Fe_2O_5$	—	—	—	—	—	—	8.89
$MgFe_2O_4$	—	—	—	—	17.52	22.64	48.18
$Ca_4Al_2Fe_2O_{10}$	—	—	—	11.49	—	—	—
CaO	10.32	11.59	6.58	7.18	—	—	—
$CaTiO_3$	—	—	—	0.70	—	—	—

*1 Data from the GIN laboratory of the Russian Academy of Sciences.

*2 Gross composition determined by electron-beam scanning over the reaction zones of the sample using a microprobe.

*3 Composition of zone 0 corresponds to the initial refractory mixture.

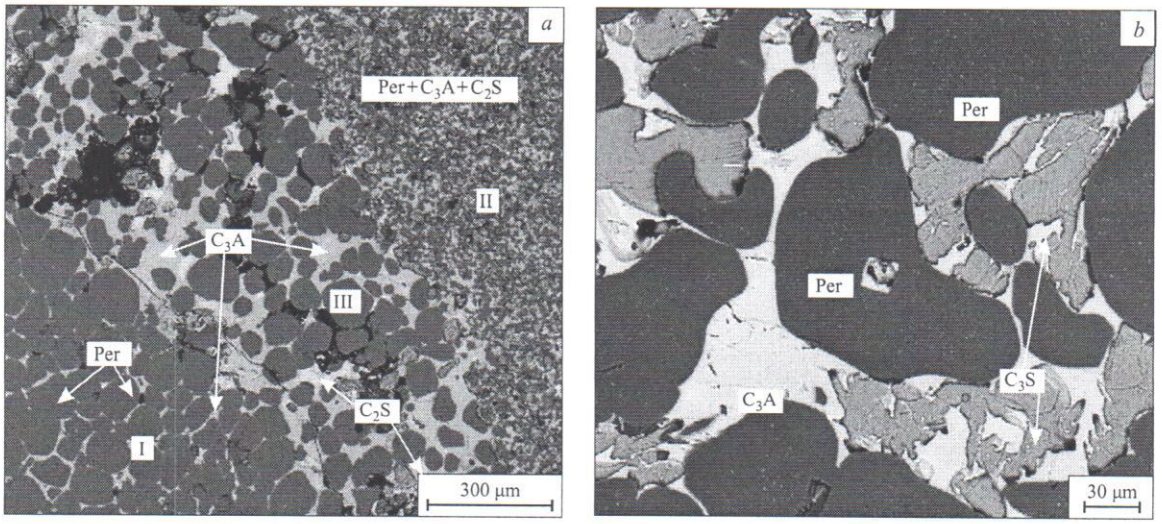

Fig. 2. Typical structure of the least altered zone 1 of the refractory mixture (sample M14). *a*) Fragments of two types with different granularity: coarse-grained (*I*) and fine-grained (*II*) consisting of dark gray periclase grains; the spaces (III) between periclase grains and between the fragments contain tricalcium aluminate (Ca_3A); C_2S is bicalcium silicate. *b*) Structure of the binder constituted by periclase grains surrounded by tricalcium aluminate and tricalcium silicate (C_3S).

fied by x-ray analysis due to their small (<5%) content in the initial materials.

Composition and Structure of Ankerharth Samples after Service

The samples taken after service from the upper part of the furnace hearth constitute well-sintered "stone-like" hard materials, frequently having a heterogeneous zonal structure due to their interaction with metallurgical melts that have a contrasting composition. The deeper in the hearth a sample was located, the less dense and the more homogenous its structure and color. At a depth of 30 cm, the cement binding larger particles becomes loose, the samples easily disintegrate into lumps, and at a depth from 40 to 60 cm the refractory is powder-like and differs from the initial material only by a darker color. The most altered samples from the furnace hearth (M14 and M14-1) have been investigated in more detail.

The initial material of sample M-14 is Ankerharth SB25B. Sample M14 is taken from the bank of the front wall near the slag belt; its height is 13 mm, its cross-section area is 15 × 16 mm, and it has clearly expressed zonality. Four reaction zones, different in their colors and textures, have been identified in this sample, in the direction of contact with metallurgical melts: 1 — light brown and 2 — yellow-brown, both having a breccia-like structure; 3 — dark brown and 4 — black, having a more homogeneous structure but numerous large pores, especially along the boundary between the light-color and the dark-color zones.

Zone 1 is the least altered; its thickness is ~7 mm and contains two types of fragments of size from 1.5 to 4.5 mm (Fig. 2*a*). Some of them differ from the light brown background of the zone; they are dark gray periclase grain aggregates of average size 0.10 – 0.12 mm, arranged close to each other, virtually clear and isotropic. The spaces between the periclase grains are filled by tricalcium aluminate and small quantities of bicalcium silicate (Table 2). Approximately 20 – 25% of the volume is taken by the second type of fragments, of an irregular, frequently angular shape, from 3 × 2 to 9 × 5 mm, consisting of significantly smaller periclase grains (10 – 20 μm or less). The spaces between them are filled not only by tricalcium aluminate but also by lime CaO in the form of rounded formations (Fig. 2*a*) with very fine prismatic crystals of portlandite $Ca(OH)_2$ visible along the contour. The binding material between the two types of fragments consists of periclase grains of an isometric, often faceted shape. The grain size varies from 6 – 10 to 200 – 300 μm. The iron content in it amounts to fractions of a percent. The space between the periclase grains are filled by tricalcium aluminate with Mg, Mn, Fe, Ti, and Si impurities and tricalcium silicate with Mg, Mn, Fe, and Ti impurities (Fig. 2*b*); bicalcium silicate and braunmillerite $Ca_4Al_2Fe_2O_{10}$ are found in small quantities (Table 2).

The differences between the two types of fragments become less pronounced nearer to the contact between the refractory and the melt. At a distance of about 8 mm from dark zone 3, the quantity of free CaO decreases; C_3S and C_3A disappear and are replaced by C_2S. This characteristic was used to identify zone 2 of thickness ~1 mm. Periclase in zone 2 contains numerous fine inclusions of magnesioferrite. Its ferrous coefficient grows to 0.15 compared to $f = 0.08$ in zone 1 (Table 2). The boundaries of the periclase grains become smoother and more rounded. The quantity of the binding material made up of bicalcium silicate grows compared to the

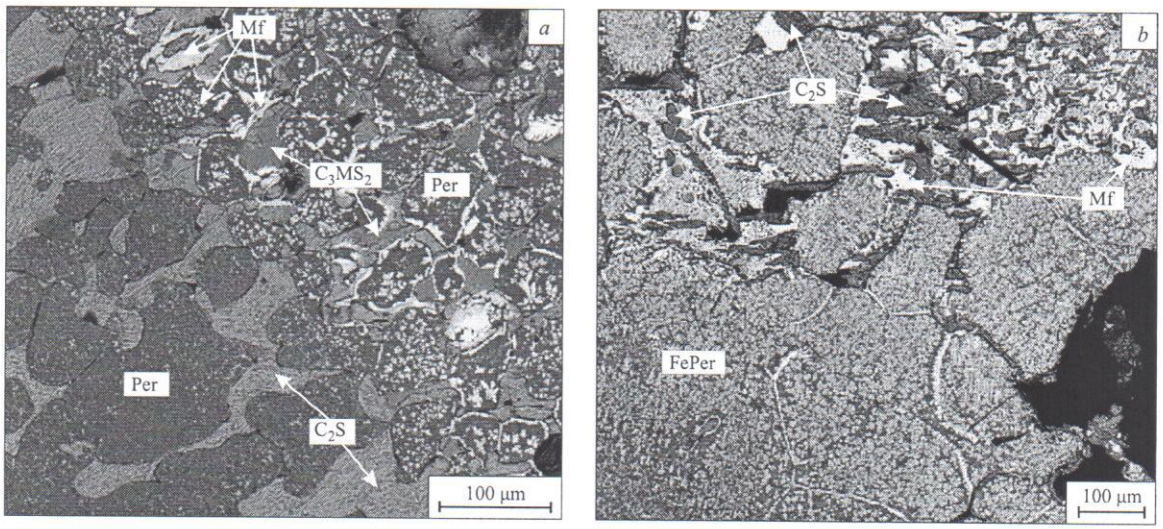

Fig. 3. Contact areas between reaction zones in sample M14. *a*) A sharp boundary between zones 2 (left) and 3 manifested in altered structure and mineral composition. Composition of zone 2: Per + C_2S, zone 3: ferrous periclase and magnesioferrite (Mf) + mervinite (C_3MS_2). *b*) At the contact of zone 3 (left) and zone 4, the phases of zone 3 are replaced by zone 4 minerals. The material contains light-colored, banded, and cellular Mf formations and lens-like C_2S veinlets.

material in zone 1. This is related to a partial removal of Mg, the contribution of Si, and filling this space by C_2S. Its composition (Table 2) has small impurities of iron, manganese, and phosphor. The electron photos show its heterogeneous,

TABLE 2. Crystallochemical Formulas of Phases Split by Reaction Zones of the Hearth in Sample M14 (initial material*1 Ankerharth SB25)

Analysis number	Zone	Distance, mm	Phase	Ferrous coefficient *f*	Phase composition
46	1	83 – 513	Per	0.08	$(Mg_{0.91}Ca_{0.01}Fe_{0.08})O$
48	1	83 – 513	C_3S	0.08	$(Ca_{3.02}Mg_{0.03})_{3.05}(Si_{0.87}Al_{0.04}Fe_{0.05}Ti_{0.02}P_{0.01})_{0.99}O_5$
47	1	83 – 513	C_3A	0.08	$(Ca_{2.60}Mg_{0.18}Mn_{0.01}Fe_{0.30})_{3.09}(Al_{1.14}Fe_{0.55}Ti_{0.21}Si_{0.10})_{2.00}O_6$
41	2	73 – 58	Per*2	0.15	$(Mg_{0.80}Fe_{0.15}Mn_{0.05})_{0.98}O$
42	2	73 – 58	C_2S	0.15	$(Ca_{1.96}Mg_{0.10}Mn_{0.01})_{2.07}(Si_{0.90}Fe_{0.01}P_{0.04})_{0.95}O_4$
43, 38	3	23 – 57	Per	0.20	$(Mg_{0.76}Fe_{0.19}Mn_{0.04})_{0.90}O$
34	3	23 – 57	Per*2	0.43	$(Mg_{0.51}Al_{0.02}Fe_{0.39}Mn_{1.05})_{1.06}O$
44, 40, 37*2	3	23 – 57		0.75	$(Mg_{0.76}Ca_{0.09}Mn_{0.21})_{1.06}(Fe_{2.34}Al_{0.31}Ti_{0.02}Si_{0.01})_{2.08}O_4$
45	3	23 – 57	C_3MS_2	—	$(Ca_{3.09}Na_{0.01})_{3.10}(Mg_{0.92}Fe_{0.07})_{1.01}(Si_{1.90}Al_{0.01}Ti_{0.01}P_{0.02})_{1.94}O_8$
39	3	23 – 57	C_2S	—	$(Ca_{2.17}Mg_{0.02}Na_{0.01})_{2.20}(Si_{0.78}Fe_{0.01}P_{0.01})_{0.80}O_4$
31	3	23 – 57	Per	0.12	$(Mg_{0.860}Fe_{0.12}Mn_{0.02})O$
32	3	23 – 57	C_2S	—	$(Ca_{2.07}Mg_{0.01}Na_{0.02})_{2.10}(Si_{0.89}Al_{0.02})_{0.91}O_4$
33	3	23 – 57	C_4AF	0.96	$(Ca_{4.61}Mg_{0.09}Mn_{0.06})_{4.76}(Al_{1.53}Si_{0.09}P_{0.01})_{1.63}(Fe_{2.60}Ti_{0.06})_{2.66}O_{10}$
35	4	03 – 52	Mf	0.79	$(Mg_{0.69}Ca_{0.07}Mn_{0.13}Ti_{0.03})_{0.92}(Fe_{2.60}Al_{0.22})_{2.86}O_4$
36	4	03 – 52	C_2S	—	$(Ca_{1.97}Na_{0.01})_{1.98}(Si_{0.97}P_{0.01}Fe_{0.02})_{1.00}O_4$
29	4	03 – 52	Mf	0.63	$(Mg_{1\cdot26}Ca_{0.06}Mn_{0.21}Na_{0.02})_{1.55}(Fe_{2.16}Al_{0.010}Si_{0.02}Ti_{0.01})_{2.35}O_4$
30, 23			Per (border)	0.29	$(Mg_{0.66}Fe_{0.27}Mn_{0.06})_{0.99}O$
24	4	03 – 52	Per (center)	0.45	$(Mg_{0.49}Ca_{0.01}Fe_{0.41}Al_{0.01}Mn_{0.05})_{0.97}O$
25, 26, 21	4	03 – 52	Mf	0.80	$(Mg_{0.67}Ca_{0.07}Mn_{0.21})_{0.95}(Fe_{2.63}Al_{0.28})_{2.91}O_4$
28, 27	4	03 – 52	C_2S	—	$(Ca_{1.86}Mg_{0.16}Mn_{0.01}Fe_{0.04})_{2.07}(Si_{0.89}Al_{0.01}P_{0.03})_{0.93}O_4$
22	4	03 – 52	C_2S	—	$(Ca_{2.04}Mg_{0.01}Na_{0.01})_{2.06}(Si_{0.94}Fe_{0.03}P_{0.02})_{0.99}O_4$

*1 The phase composition of the initial material (distance from the contact with molten metal >18 mm) Per + C_3S + C_2F + C_3A + CaO. Phase notations: Per, MgO (Periclase); C_3S, $3CaO \cdot SiO_2$; C_2F, $2CaO \cdot Fe_2O_3$; C_3A, $3CaO \cdot Al_2O_3$; C_2S, $2CaO \cdot SiO_2$; $C_3MS_23 - 53CaO \cdot MgO \cdot 2SiO_2$; C_4AF, $4CaO \cdot Al_2O_3 \cdot Fe_2O_3$; Mf, $MgO \cdot Fe_2O_3$.

*2 Scanning surface area 20 × 20 μm.

*3 The mean value of several results of analysis.

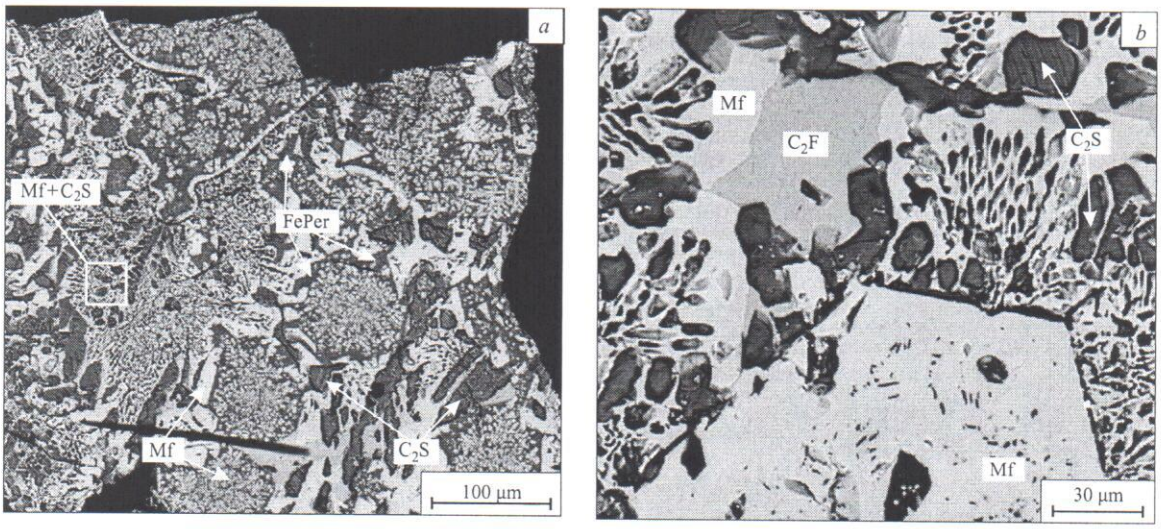

Fig. 4. Typical structure of zone 4. *a*) Mf manifested as skeleton and dendrite forms inside ferrous periclase grains and formation of edge borders and angular crystals in the peripheral parts of the grains (sample No. 14); *b*) magnesioferrite crystals of hexahedral and cellular shapes, the spaces between them are filled by rounded and lens-like C_2S formations (sample M14-1).

seemingly fibrous structure (Fig. 3*a*). A clearly defined boundary is visible between zone 2 and the two successive (zones 3 and 4) dark-colored and most altered zones. The color, structure, and mineral composition of the refractory material are modified.

Zone 3 (dark brown) is ~5 mm thick. The quantity of magnesioferrite in periclase grains and along their contacts with other phases significantly grows, and magnesioferrite pseudomorphoses are formed over periclase. The spaces between the periclase grains are filled by bicalcium silicate and a new phase, i.e., mervinite $Ca_3MgSi_2O_8$ (Fig. 3*a*). The size of mervinite formations ranges from 10 to 100 μm. It contains Fe, Al, Ti, Mn, and P impurities. Braunmillerite is present in this zone in small quantities. The formation of mervinite indicates a deficit of calcium and its perceptible loss by the refractory, starting with zone 3. This process is also manifested by the disappearance of free CaO. Bicalcium silicate also contains MgO, whose quantity grows from 0.4 in zone 1 to 4.5 wt.% in zone 4. Apparently, C_2S is stabilized by the incorporation of Mg. The stability of Mg-bearing C_2S is confirmed by the existence of a natural mineral with a similar composition, namely bredigite (α'-Ca_2SiO_2) containing up to 6.4 wt.% MgO, which has been discovered in lime scarns in Ireland [8]. Bicalcium silicate contains small quantities of P_2O_5: from 0.3 to 1.5 wt.%, which also stabilizes this mineral in the high-temperature form.

Zone 4 (black color) is ~2 mm thick. It is separated from zone 3 by a sharp tortuous border, which is clearly seen in Fig. 3*b*. Large periclase grains, whose volume is saturated with fine magnesioferrite dendrites, are visible at the edges of zone 3; magnesioferrite also fills the cracks at the boundaries of the periclase grains. On the border between zones 3 and 4, periclase is intensely replaced by light-colored, banded, and clear magnesioferrite formations; the spaces between them are filled by lens-shaped bicalcium silicate penetrating along the cracks and periclase grain contacts. The substitution process is accompanied by pore formation. The structural differences between the coarse-grained and close-grained aggregates, which can be observed in zones 1 and 2, here completely disappear. Periclase in zone 4 consists of nearly black opaque grains with brown translucence at the edges. The reflected-light microscopy and backward-scattered electron photos (Fig. 4*a*) reveal not only numerous skeleton magnesioferrite formations over periclase, but also the fact that the edges of periclase grains are replaced by magnesioferrite in the form of wide (20 – 30 μm) edge borders and angular crystals with sharp faces of size up to 70 μm. The quantity of magnesioferrite grows significantly (up to 40%). Relict periclase grains recrystallize at their edges and "lose" part of the iron ($f = 0.29$), which is incorporated in large magnesioferrite crystals. Their central parts remain saturated with iron ($f = 0.45$) and correspond to the composition of magnesiowustite. The content of Al and Mn in periclase grains grows. Elongated bicalcium silicate formations of size 30 – 100 μm are seen between the grains. Mervinite is not identified in zone 4. Magnesioferrite has a significantly higher content of aluminum. Thus, zone 4 consists of three main minerals: ferrous periclase (magnesiowustite), magnesioferrite, and bicalcium silicate. The cellular structures formed by Mf and having C_2S inside suggest that a melt (containing ferrous and silicate phases) might be formed in zone 4, as a consequence of chemical reactions between the refractory and the metallurgical melt.

It is interesting to compare the results of the interaction of the same metallurgical melt with another grade of refractory ramming mixture, i.e., Ankerharth TLS2 (sample M14-1), which differs from Ankerharth SB25 by a lower

TABLE 3. Crystallochemical Formulas of Phases Split by Reaction Zones in Sample M14-1 (initial material Ankerharth TLS2, analysis M16)

Analysis number	Zone	Distance, mm	Phase	f	Phase composition
M-16	0	>30	Per	0.02	$(Mg_{0.97}Ca_{0.01}Fe_{0.02})_{1.00}O$
M-16	0	>30	C_3F	—	$(Ca_{2.82}Mg_{0.10}Mn_{0.06}Ti_{0.01}P_{0.13})_{3.12}(Fe_{2.01}Al_{0.16}Si_{0.23})_{2.40}O_6$
14-1-7, 3	1	10 – 18	Per	0.01	$(Mg_{1.03}Ca_{0.01}Fe_{0.01})_{1.05}O$
1	1	10 – 18	CaO	—	$(Ca_{0.92}Fe_{0.04}Mg_{0.03}Mn_{0.01})_{1.00}O$
1a	1	10 – 18	(Cs, Mg)O	—	$(Ca_{0.73}Mg_{0.24}Fe_{0.03}Mn_{0.01})_{1.01}O$
2, 5	1	10 – 18	C_4AF	—	$(Mg_{0.26}Ca_{4.27}Mn_{0.02})_{4.55}(Al_{1.81}Si_{0.18})_{1.00}(Fe_{1.58}Ti_{0.39})_{1.97}O_{10}$
4	1	10 – 18	Ca_3SiO_5	—	$(Ca_{2.98}Mg_{0.04}Fe_{0.06})_{3.08}(Si_{0.88}Al_{0.04}Ti_{0.03})_{0.95}O_4$
7	1	10 – 18	$Ca_2Fe_2O_5$	—	$(Ca_{2.44}Mg_{0.03}Mn_{0.02})_{2.49}(Fe_{2.21}Al_{0.10}Si_{0.02})_{2.26}O_5$
6	1	10 – 18	Fo?	—	$(Mg_{1.24}Fe_{0.05})_{1.29}(Si_{0.82}Al_{0.55})_{1.37}O_4$
14-1-6, 1	1	10 – 18	Ca_3SiO_5	—	$(Ca_{2.98}Mg_{0.02}Fe_{0.03}Mn_{0.01}Na_{0.01})_{3.05}(Si_{0.91}Al_{0.04})_{0.95}O_5$
2	1	10 – 18	$Ca_3Fe_2O_6$	—	$(Ca_{2.85}Mg_{0.12}Mn_{0.07})_{3.04}(Fe_{1.54}Al_{0.64}Si_{0.16})_{2.41}O_6$
3	1	10 – 18	Per	0.06	$(Mg_{0.92}Ca_{0.01}Mn_{0.01}Fe_{0.06})_{1.0}O$
4, 5	1	10 – 18	CaO	—	$(Ca_{0.8}Mg_{0.06}Mn_{0.02}Fe_{0.03})_{0.91}O$
14-1-5, 5	2	4.5 – 10	Per	0.15	$(Mg_{0.80}Mn_{0.03}Fe_{0.14})_{0.97}O$
1	2	4.5 – 10	$Ca_3Fe_2O_6$	—	$(Ca_{2.70}Mg_{0.06}Ti_{0.14}Mn_{0.08})_{2.98}(Fe_{1.89}Al_{0.39}Si_{0.19})_{2.47}O_6$
2	2	4.5 – 10	Mf (with Mn)	0.11	$(Mg_{0.77}Cs_{0.08}Mn_{0.19})_{1.04}(Fe_{2.34}Al_{0.36}Co_{0.02})_{2.72}O_4$
3	2	4.5 – 10	Ca_2SiO_4	—	$(Ca_{2.02}Fe_{0.01}Ti_{0.01}Mg_{0.01}Na_{0.01})_{2.06}Si_{0.95}O_4$
0	2	4.5 – 10	Per (by S)	0.18	$(Mg_{0.58}Al_{0.01}Si_{0.06}Ca_{0.12}Mn_{0.02}Fe_{0.13})_{0.92}O$
14-1-4, 2	3	3.5 – 4.5	Mf	0.75	$(Mg_{0.77}Ca_{0.05}Ti_{0.02}Mn_{0.20}Na_{0.01})_{1.05}(Fe_{2.33}Al_{0.32})_{2.65}O_4$
1	3	3.5 – 4.5	$Ca_2Fe_2O_5$	—	$(Ca_{1.98}Mg_{0.07}Mn_{0.06})_{2.11}(Fe_{1.05}Al_{0.20}Si_{0.27}Ti_{0.48})_{2.00}O_5$
4, 7, 8	3	3.5 – 4.5	Per	0.19	$(Mg_{0.77}Mn_{0.02}Fe_{0.18})_{0.97}O$ (by S 500 × 500)
6	3	3.5 – 4.5	Ca_2SiO_4	—	$(Ca_{1.98}Fe_{0.03}Mn_{0.01}Ti_{0.01}Na_{0.01})_{2.04}Si_{0.97}O_4$
14-1-2, 1, 3, 5, 9	4	0 – 3.5	Mf	0.80	$(Mg_{0.74}Ca_{0.07}Mn_{0.19})_{0.90}(Fe_{2.60}Al_{0.10}Ti_{0.01})_{2.71}O_4$
4, 7, 8	4	0 – 3.5	Per	0.28	$(Mg_{0.66}Mn_{0.04}Fe_{0.20})_{0.90}O$
2	4	0 – 3.5	Ca_2SiO_4	—	$(Ca_{1.98}Fe_{0.02}Ti_{0.07})_{2.07}(Si_{1.00}Al_{0.01})_{1.01}O_4$
6	4	0 – 3.5	$Ca_2Fe_2O_5$	—	$(Ca_{2.31}Mg_{0.04}Ti_{0.06}Mn_{0.06})_{2.47}(Fe_{1.90}Si_{0.14}Al_{0.18})_{2.22}O_5$

*1 Forsterite.

content of MgO and a higher content of CaO and FeO. The sample M14-1 taken from the upper part of the blow zone of the hearth near the central lance has clearly expressed zonality, generally resembling the zonality of sample M14, but with some peculiarities. For this sample we have got not only its phase compositions (Table 3) but also the gross compositions of the materials split by reaction zones (Table 1), which were obtained by microprobe analysis using electron beam scanning.

Four zones differing in their color, structure, and thickness have been identified in sample M14-1. The structure of the first two zones is breccia-like, similarly to sample M14. The main mineral in zone 1 of thickness 8 mm is periclase as well. The ferrous factor of periclase grows from 0.01 at the beginning to 0.06 at the end of the zone. This zone contains lime, sometimes magnesium-bearing lime (Table 1). The periclase-binding material in zone 1 of sample M14-1 mainly contains braunmillerite, as well as small quantities of tricalcium silicate and bi- and tricalcium ferrites (Table 3), thus differing from the binder in sample M14, where the main mineral is tricalcium aluminate. The mineral norm of zone 1 calculated on the basis of the chemical composition (Table 1) mainly coincides with the estimate obtained using the microprobe.

Zone 2 of thickness 5.5 mm consists of periclase and a binding material consisting of C_2S and C_3F. Periclase is saturated with iron ($f \sim 0.15$) and starts to be replaced by magnesioferrite containing up to 0.2 formula units of Mn and 0.3 formula units of Al (Table 3). The pores in zone 2 are larger (500 – 700 μm) than in zone 1. They are frequently surrounded by edge borders containing magnesioferrite and tricalcium ferrite, whose quantity grows in approaching zone 4. The calculation of the mineral norm of this zone mainly confirms the data of microprobe analysis.

Zones 3 and 4 are separated from zones 1 and 2 by a clearly defined boundary: the color of the refractory turns dark brown and at the site of contact with the melt it becomes black; the breccia-type structure is replaced by a denser and more homogeneous texture; the emergence of large round and slot-like pores is registered along the boundary.

Zone 3 of thickness 1 mm contains periclase, whose ferrous factor is increased to 0.23, and an increased quantity of magnesioferrite in the form of dendrites in the periclase and border edges between the grains. Aggregates consisting of C_2S, C_2F, and Mf of size up to 100 μm are identified along the cracks and the pores. Converted to the norm, the majority of calcium in zone 3 is contained in bicalcium silicate; bivalent iron is contained in periclase, and trivalent iron in

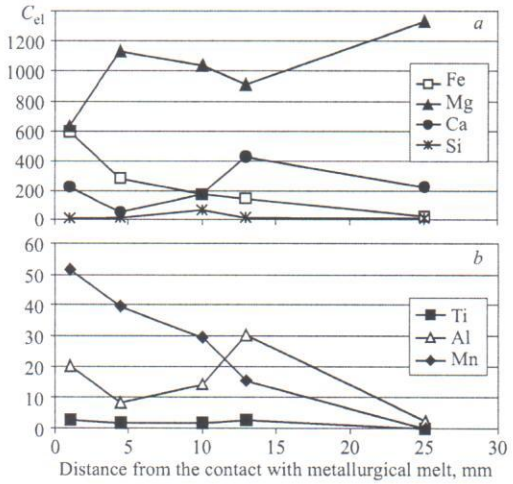

Fig. 5. Variations in the gross composition of refractory Ankerharth TLS_2 depending on the distance from the contact with metal melt downwards into the hearth towards the unaltered refractory (sample M14-1); *a*) atomic quantities of Fe, Mg, Ca, Si; *b*) Ti, Al, Mn; C_{el}, concentration of the element (number of cations per 1600 atoms of O).

magnesioferrite. In contrast to sample M14, mervinite is not found in zone 3 of sample M14-1.

Zone 4 is black-colored of thickness 3.5 mm and clearly separated from zone 3. It has a significantly lower (25%) content of periclase, which corresponds to magnesiowustite ($f = 0.3$) in the center of the grains. The quantity of magnesioferrite grows to 50%. It forms not only dendrites, border edges, and veinlets in the periclase, but also individual idiomorphic crystals up to 150 μm in size (Fig. 4*b*), yielding hexahedral and trapezoidal sections. Bicalcium ferrite (around 8%) exists in close accretions with magnesioferrite. The spaces between magnesioferrite and bicalcium ferrite dendrites are filled by crystallizing C_2S (about 17%). The mineral composition of the zone which is the nearest to the melt in M14-1 is nearly identical to the same zone in sample M14. The difference consists of a larger quantity of bicalcium ferrite in sample M14-1.

Zonal variations of the gross composition of sample M14-1 calculated in atomic quantities of elements per 1600 oxygen atoms (Fig. 5) make it possible to observe the behavior of each component in the formation of reaction zones between the refractory material and the metallurgical melt.

Iron diffuses from the furnace chamber and is monotonically accumulated in consecutive zones. The FeO content grows from 2.5 wt.% in the initial refractory to 15 wt.% in the end of zone 1 and to 50 wt.% in zone 4. Calcium ferrites are the first to be formed, the next is braunmillerite at $Al_2O_3 > 3\%$, and then magnesioferrite. Meanwhile, periclase becomes saturated with iron oxides and its ferrous factor increases, the nearer the melt. Simultaneously with the contribution of iron, magnesium is removed from the refractory into the workspace of the furnace; the content of MgO decreases sharply from 74 wt.% in the initial mixture to 43 wt.% in the end of zone 1 and to 23% in zone 4 contacting the melt. The diffusion process is accompanied by an increase in f of periclase and a growing quantity of magnesioferrite in the refractory composition. The amount of FeO sharply increases and the content of MgO decreases in zone 4, which is the nearest to the melt.

CaO is nonuniformly distributed among the zones; its maximum content (~34 wt.%) is registered at the border between zones 1 and 2. Such an increased quantity of CaO in zone 2 is presumably related to the most intense removal of MgO. Calcium is registered in this zone as part of tricalcium silicate, ferrite, and braunmillerite and also exists in the free form as lime. Moving toward the contact with the melt, the content of CaO drops to 4.3 wt.% in zone 3, in which free CaO disappears. The content of CaO grows again in contact zone 4, presumably due to the contribution of calcium from the slag melt into the refractory. The CaO/SiO_2 ratio perceptibly decreases as well: from 35 in the initial refractory material to approximately 2 in the reaction zones.

The content of SiO_2 grows from 0.6% in the initial samples to 6.4% in zone 4 adjacent to the metallurgical melt. A significant accumulation of SiO_2 is observed in zone 2 (7.8%), which is located at a distance of from 4.5 to 10 mm from the contact with the melt. Silica mostly makes up part of the calcium silicates, whose composition depends on the presence of free CaO and the CaO/SiO_2 ratio. When free CaO disappears, tricalcium silicate transforms into bicalcium silicate. Calcium silicates are present in all zones: tricalcium silicate in zones 1 and 2 and bicalcium silicate in zones 3 and 4.

The accumulation of Al_2O_3, similarly to CaO, is observed within zone 1 (up to 3 wt.%). Aluminum makes up parts of braunmillerite and in more altered zones is part of magnesioferrite. It is assumed that aluminum may be contributed both by the metallurgical melt and by the chamotte bricks underlying the hearth, since its quantity in the initial ramming mixture is insignificant: less than 1 wt.%.

Manganese is contributed to the refractory from the melt and is accumulated up to 4.4 wt.% MnO in reaction zones 3 and 4, its quantity gradually decreasing towards the less altered zones.

Manganese participates in the formation of magnesioferrite crystals, isomorphically replacing Mg.

CONCLUSIONS

The results of studying Ankerharth magnesian-dolomite ramming mixtures after service corroborate the known proposition that corrosion caused by chemical reactions in service is the deciding factor in lowering the resistance of refractory ramming mixtures in open-hearth furnaces. General regularities of changes in refractories are identified, which are manifested in zonality at the interface of two media: the refractory and the metallurgical melt. Four zones are identified: from

the least altered (zone 1), whose phase composition is the closest to the initial refractory mixture, to a fundamentally altered zone (zone 4), which almost totally consists of newly formed phases.

The total thickness of the considered samples reaches a few tens of millimeters, the thickness of the most altered zone being 5 – 8 mm. It varies depending on such factors as the initial mixture composition, the location in the furnace hearth and, presumably, the duration of service of the refractories. The main features in the modification of refractory composition are the removal of magnesium and the contribution of iron, silicon, titanium, and manganese from metallurgical slag. The emerging zones have clearly defined boundaries determined by the formation or disappearance of a particular phase and significant alteration of the composition and quantitative ratios of phases. As the process intensity grows from one zone to another, the emerging phases become fewer.

The general regularities of zonal variations of the mineral composition of Ankerharth SB25 and Ankerharth TLS2 mixtures toward the contact with metallurgical melts are as follows: an increasing ferrous factor $f = Fe/(Fe + Mg)$ of periclase and formation of magnesiowustite, replacement of periclase by magnesioferrite and then complete disappearance of free CaO, and replacement of tricalcium silicate by bicalcium silicate in the most intensely transformed zones.

The differences between the considered refractories after service are more evident in the zones most remote from the metal contact and in the middle zones. In Ankerharth SB25, tricalcium aluminate and tricalcium silicate prevail in the periclase-binding material of the first zone and mervinite and bicalcium silicate prevail in the middle zones, whereas Ankerharth TLS2 typically contains braunmillerite, calcium ferrites, and bicalcium silicate in these zones.

In zone 4, which is the nearest to metallurgical melts, the compositions of both refractories become nearly identical. Periclase persists only as relict grains with a high ferrous content (30 – 45%), magnesioferrite and bicalcium silicates are present in large quantities, and bicalcium ferrite is found in small quantities. Typical cellular structures are formed by elongated thin (branched) magnesioferrite crystals; between them are contained lens-like bicalcium silicate formations, which is interpreted by us as a manifestation of a liquid phase probably existing between the large magnesiowustite grains at high temperatures. The formation of such a melt might facilitate the softening of the refractory surface and its erosion. The refractoriness of materials is significantly impaired by new minerals formed in solid-phase reactions: calcium and magnesium silicates, aluminates, and ferrites, which are not found in the initial refractories. The resistance of refractories is also decreased by the formation of numerous pores at the border between the intensely altered zones (the black crust) and the underlying least altered light-color zones, as a consequence of volumetric changes during the recrystallization of the refractory and the shrinkage of materials. This reaction crust may become exfoliated, after which the refractory undergoes further destruction.

REFERENCES

1. D. S. Korzhinskii, "Granitizing as magmatic substitution," *Izv. AN SSSR. Ser. Geol.*, No. 2, 56 – 59 (1952).
2. E. N. Gramenitskii, T. I. Shchekina, A. B. Batanova, et al. "A study of liquid-phase interaction of chromite-periclase refractories with aggressive media in producing nickel converter matte," *Nov. Ogneupory*, No. 8, 25 – 32 (2005).
3. E. N. Gramenitskii, A. B. Batanova, et al. "A model of interaction between a refractory and a glass-forming melt," *Dokl. RAN*, **356**(6) (1997).
4. E. N. Gramenitskii, T. I. Shchekina, A. B. Batanova, et al. "Emergence of zonality in reactions between a granite melt and pyroxenite," *Vestnik MGU Geol.*, No. 3, 27 – 37 (2001).
5. E. N. Gramenitskii, A. B. Batanova, T. I. Shchekina, et al. "Mechanisms of assimilation and magmatic substitution," *Izv. RAEN Earth Sci. Sec.*, Issue 8, 50 – 63 (2002).
6. L. I. Karyakin, *Petrography of Refractories* [in Russian], Kharkov (1962).
7. D. S. Belyankin, B. V. Ivanov, and V. V. Lapin, *Petrography of Technical Stone* [in Russian], Moscow, AN SSSR (1952).
8. S. M. Aleksandrov, "Genesis and mineral composition of lime skarns from progressive and regressive metasomatism stages," *Geokhimiya*, No. 3, 281 – 297 (2002).